JVI Journals.ASM.org

# Coronavirus nsp10/nsp16 Methyltransferase Can Be Targeted by nsp10-Derived Peptide *In Vitro* and *In Vivo* To Reduce Replication and Pathogenesis

**Yi Wang,[a] Ying Sun,[b] Andong Wu,[a] Shan Xu,[a] Ruangang Pan,[a] Cong Zeng,[a] Xu Jin,[a] Xingyi Ge,[c] Zhengli Shi,[c] Tero Ahola,[d] Yu Chen,[a] Deyin Guo[a]**

State Key Laboratory of Virology, College of Life Sciences, Wuhan University, Wuhan, China[a]; Department of Pathogen Biology, Henan University of TCM, Zhengzhou, China[b]; Center for Emerging Infectious Diseases, State Key Laboratory of Virology, Wuhan Institute of Virology, Chinese Academy of Sciences, Wuhan, China[c]; Department of Food and Environmental Sciences, University of Helsinki, Helsinki, Finland[d]

**ABSTRACT**

**The 5′ cap structures of eukaryotic mRNAs are important for RNA stability and protein translation. Many viruses that replicate in the cytoplasm of eukaryotes have evolved 2′-*O*-methyltransferases (2′-*O*-MTase) to autonomously modify their mRNAs and carry a cap-1 structure (m7GpppNm) at the 5′ end, thereby facilitating viral replication and escaping innate immune recognition in host cells. Previous studies showed that the 2′-*O*-MTase activity of severe acute respiratory syndrome coronavirus (SARS-CoV) nonstructural protein 16 (nsp16) needs to be activated by nsp10, whereas nsp16 of feline coronavirus (FCoV) alone possesses 2′-*O*-MTase activity (E. Decroly et al., J Virol 82:8071–8084, 2008, http://dx.doi.org/10.1128/JVI.00407-08; M. Bouvet et al., PLoS Pathog 6:e1000863, 2010, http://dx.doi.org/10.1371/journal.ppat.1000863; E. Decroly et al., PLoS Pathog 7:e1002059, 2011, http://dx.doi.org/10.1371/journal.ppat.1002059; Y. Chen et al., PLoS Pathog 7:e1002294, 2011, http://dx.doi.org/10.1371/journal.ppat.1002294). In this study, we demonstrate that stimulation of nsp16 2′-*O*-MTase activity by nsp10 is a universal and conserved mechanism in coronaviruses, including FCoV, and that nsp10 is functionally interchangeable in the stimulation of nsp16 of different coronaviruses. Based on our current and previous studies, we designed a peptide (TP29) from the sequence of the interaction interface of mouse hepatitis virus (MHV) nsp10 and demonstrated that the peptide inhibits the 2′-*O*-MTase activity of different coronaviruses in biochemical assays and the viral replication in MHV infection and SARS-CoV replicon models. Interestingly, the peptide TP29 exerted robust inhibitory effects *in vivo* in MHV-infected mice by impairing MHV virulence and pathogenesis through suppressing virus replication and enhancing type I interferon production at an early stage of infection. Therefore, as a proof of principle, the current results indicate that coronavirus 2′-*O*-MTase activity can be targeted *in vitro* and *in vivo*.**

**IMPORTANCE Coronaviruses are important pathogens of animals and human with high zoonotic potential. SARS-CoV encodes the 2′-*O*-MTase that is composed of the catalytic subunit nsp16 and the stimulatory subunit nsp10 and plays an important role in virus genome replication and evasion from innate immunity. Our current results demonstrate that stimulation of nsp16 2′-*O*-MTase activity by nsp10 is a common mechanism for coronaviruses, and nsp10 is functionally interchangeable in the stimulation of nsp16 among different coronaviruses, which underlies the rationale for developing inhibitory peptides. We demonstrate that a peptide derived from the nsp16-interacting domain of MHV nsp10 could inhibit 2′-*O*-MTase activity of different coronaviruses *in vitro* and viral replication of MHV and SARS-CoV replicon in cell culture, and it could strongly inhibit virus replication and pathogenesis in MHV-infected mice. This work makes it possible to develop broad-spectrum peptide inhibitors by targeting the nsp16/nsp10 2′-*O*-MTase of coronaviruses.**

The 5′ ends of eukaryotic cellular mRNAs and most viral mRNAs possess a cap structure, which plays important roles in mRNA splicing, intracellular RNA transport, RNA stability, and translation initiation (1). Host and viral RNA molecules lacking the 5′ cap structure are rapidly degraded in the cytoplasm (2). The cap-0 structure of mRNA is cotranscriptionally formed through sequential enzymatic reactions, including RNA triphosphatase (TPase), RNA guanylyltransferase (GTase), and RNA (guanine-N7)-methyltransferase (N7-MTase) (1). In higher eukaryotes and some viruses, cap-0 structure m7GpppN-RNA is further methylated at the ribose 2′-*O* position of the nascent mRNA by a ribose 2′-*O*-methyltransferase (2′-*O*-MTase) to form a cap-1 structure (m7GpppNm) and cap-2 structure (m7GpppNmNm). Both N7-MTase and 2′-*O*-MTase can catalyze the transfer of the methyl group from the methyl donor S-adenosyl-L-methionine (SAM or AdoMet) to RNA substrate and generate *S*-adenosyl-L-homocysteine (SAH or AdoHcy) as a by-product. The functions of viral RNA cap structure include the following: (i) the guanosine cap core structure protects the 5′-triphosphate from activating the host innate immune response (3, 4); (ii) the N7 methylation is essential for viral replication through the enhancement of viral RNA translation (5); and (iii) the 2′-*O* methylation functions to

**Received** 12 April 2015 **Accepted** 26 May 2015

**Accepted manuscript posted online** 3 June 2015

**Citation** Wang Y, Sun Y, Wu A, Xu S, Pan R, Zeng C, Jin X, Ge X, Shi Z, Ahola T, Chen Y, Guo D. 2015. Coronavirus nsp10/nsp16 methyltransferase can be targeted by nsp10-derived peptide *in vitro* and *in vivo* to reduce replication and pathogenesis. J Virol 89:8416–8427. doi:10.1128/JVI.00948-15.

**Editor:** S. Perlman

Address correspondence to Yu Chen, chenyu@whu.edu.cn, or Deyin Guo, dguo@whu.edu.cn.

Y.W. and Y.S. contributed equally to this work.



doi:10.1128/JVI.00948-15

evade the recognition of host RNA sensors, such as RIG-I, Mda-5, and IFIT, and to resist the interferon (IFN)-mediated antiviral response (6, 7). Since many RNA viruses replicate in the cytoplasm, they cannot access the host capping machinery located in the nucleus. Therefore, most of them have evolved to encode their own capping apparatus. The critical role of viral RNA cap structure and the distinct mechanisms of host and viral RNA capping formation have opened new opportunities for vaccine and antiviral drug development (8, 9).

Coronaviruses (CoVs) are common pathogens of respiratory, gastrointestinal, hepatic, and central nervous system diseases of humans and animals (10). It has been reported that bats are natural carriers of coronaviruses (11–13) and that coronaviruses may be transmitted from animals to humans, as exemplified by severe acute respiratory syndrome coronavirus (SARS-CoV) and Middle East respiratory syndrome coronavirus (MERS-CoV) (14). Therefore, coronaviruses are important pathogens that threaten human health and economy. The *Coronavirinae* subfamily is classified into four genera, including *Alphacoronavirus*, *Betacoronavirus*, *Gammacoronavirus*, and *Deltacoronavirus* (15). The classification originally was based on antigenic relationships and later confirmed by sequence comparisons of entire viral genomes (16). Coronaviruses are enveloped, positive-sense single-stranded RNA viruses. The 5′-terminal two-thirds of the coronaviral genome contains a large open reading frame (ORF), ORF1ab, which encodes polyprotein 1a (pp1a) and polyprotein 1ab (pp1ab), the latter being generated via a −1 ribosomal frameshift (17). The polyproteins pp1a/1ab are cleaved into 16 nonstructural proteins (nsp1 to nsp16) and include many RNA-processing enzymes, such as RNA-dependent RNA polymerase (nsp12) (18, 19), RNA helicase and triphosphatase (nsp13) (20), exoribonuclease and N7-MTase (nsp14) (21–23), endonuclease (nsp15) (24), and 2′-*O*-MTase (nsp16) (25–28).

In previous studies, we and others have identified nsp14 and nsp10/16 complex of SARS-CoV as N7-MTase and 2′-*O*-MTase, respectively, both of which are involved in viral RNA methylation and formation of the cap-1 structure (23, 25–28). Structure-function analysis of SARS-CoV nsp14 revealed the characteristics of this novel N7-MTase that is associated with exoribonuclease activity in the same protein (29). Interestingly, nsp10 acts as the stimulatory factor for nsp16 by stabilizing the SAM-binding pocket and extending the substrate RNA-binding groove of nsp16, as revealed by crystallographic and biochemical studies (28). Interference of the interaction between nsp10 and nsp16 of SARS-CoV by short peptides could specifically inhibit the activity of 2′-*O*-MTase (30). However, nsp16 of feline coronavirus (FCoV) from the genus *Alphacoronavirus* was shown to methylate the cap-0 structure at the ribose 2′-*O* position of the first nucleotide of viral RNA to form the cap-1 structure in the absence of nsp10 (25). Therefore, it remains unclear whether the stimulatory effect of nsp10 on nsp16 methyltransferase is universal for all coronaviruses, and further studies on the mechanisms and characteristics of the 2′-*O*-MTase of different coronaviruses will benefit the development of antiviral inhibitors that specifically target coronaviral 2′-*O*-MTase.

In this study, we provide evidence that stimulation of nsp16 methyltransferase activity by nsp10 is a common mechanism for coronaviruses, although FCoV nsp16 alone possesses low 2′-*O*-MTase activity. We further demonstrate that nsp10 is interchangeable in the stimulatory function among different coronaviruses, and a peptide derived from the conserved interaction domain of MHV nsp10 shows a broad-spectrum inhibitory effect on 2′-*O*-MTase activity *in vitro* and during virus replication. These results have implications for designing specific anticoronaviral drugs to control the viral infection.

## MATERIALS AND METHODS

**Protein expression and purification.** The coding sequences of nsp16 and nsp10 from SARS-CoV, mouse hepatitis virus (MHV), transmissible gastroenteritis virus (TGEV), and feline coronavirus (FCoV) were PCR amplified from cDNAs of the SARS-CoV WHU strain (GenBank accession no. AY394850), MHV-A59 (GenBank accession no. AY700211.1), TGEV (GenBank accession no. AJ271965.2), and FCoV (GenBank accession no. HQ012369.1). The cDNAs of MERS-CoV nsp16 and nsp10 were chemically synthesized according to the deposited sequence of MERS-CoV (GenBank accession no. KF192507.1). The cDNAs of nsp16 or nsp10 of SARS-CoV or MHV-A59 were inserted into the NdeI and SalI sites of the vector pET30a using standard recombinant DNA techniques. The coding sequence of nsp16 or nsp10 of TGEV (kindly provided by Luis Enjuanes), FCoV (kindly provided by Peter J. M. Rottier), and MERS-CoV was cloned into the BamHI and XhoI sites of pET30a, resulting in the addition of 30 extra amino acid (aa) residues at their N termini. The plasmids for IBV expression (pDest14-IBV-nsp16 and pDest14-IBV-nsp10) were a kind gift from Eric J. Snijder.

All expression plasmids separately transformed into *Escherichia coli* BL21(DE3) cells (Novagen) were cultured at 37°C in 1 liter of Luria-Bertani (LB) medium with 50 μg/ml kanamycin or 100 μg/ml ampicillin and then induced with 0.4 mM isopropyl-β-D-1-thiogalactopyranoside (IPTG) at 16°C for 12 h. The purification of nsp16 and nsp10 with His tag of SARS-CoV, MHV-A59, MERS-CoV, TGEV, IBV, and FCoV was performed as described previously (28).

**Preparation of RNA substrates.** ATP- and UTP-initiated RNA substrates comprising 20 nucleotides ($pppAC_{20}$ and $pppUC_{20}$) were transcribed *in vitro* and purified as previously described (23, 28). Unlabeled cap-0 structure m7GpppA-RNA was prepared from transcribed RNA (pppA-RNA) by vaccinia virus capping enzyme (D1/D12) by following the manufacturer's protocol (Epicentre). The $^{32}$P-labeled cap structures (m7G*pppA-RNA; the asterisk indicates that the following phosphate was $^{32}$P labeled) used as RNA substrates and cap analogues (G*pppA, m7G*pppA, and m7G*pppAm) used as positive controls were prepared and purified as previously described (23, 29).

**Biochemical assays for MTase activity.** The MTase activity analyses were performed by thin-layer chromatography (TLC) using $^{32}$P-labeled RNA substrates or by liquid scintillation assays after the purification of the $^{3}$H-labeled substrates with DEAE-Sephadex chromatography as previously described (28, 29, 31). The protocol of the MTase assay also is available from bio-protocol (http://www.bio-protocol.org/).

**Peptide synthesis.** Based on the crystal structure and our previous study (30), short peptides (Table 1) were synthesized (Shanghai Ji'er Biochemistry) with N-terminal acetyl and C-terminal amide modifications. The N termini of TP29 (Tat-P29), TP29S (Tat-Scramble), and TP29M (Tat-P29-R93A and F96A) were fused with HIV Tat-derived peptide (YGRKKRRQRRRGSG) to increase the cell-penetrating capability of peptides. All of the peptides were purified by high-performance liquid chromatography (HPLC) and verified by mass spectrometry. The peptides were dissolved in phosphate-buffered saline (PBS) before use.

**Cells, viruses, and mice.** Rat lung epithelial cells (L2) and wild-type MHV-A59 were kindly provided by Rong Ye (Shanghai Medical School of Fudan University). L2 cells, baby hamster kidney cells (BHK-21), and Vero E6 cells were grown in Dulbecco's modified Eagle's medium (DMEM; Gibco, Invitrogen) supplemented with 10% fetal bovine serum (FBS). Virus-free C57BL/6 mice were obtained from the Center for Disease Control and Prevention of Hubei province (Wuhan, China). All mice were maintained in individually ventilated cages in biosafety level 2 (BSL-2) facilities and received care in compliance with international legal

**TABLE 1** List of short peptides designed based on MHV nsp10

| Peptide | Amino acid sequence[a] |
|---|---|
| P29 | YGGASVCIYCRSRVEHPDVDGLCKLRGKF |
| P29M (P29-R93A and F96A) | YGGASVCIYCRSRVEHPDVDGLCKLAGKA |
| P29S (scrambled P29) | VLKLSCCYDGYIRACSRVGEPVGGSDDFH |
| TP29 (Tat-P29) | *YGRKKRRQRRRGSG*YGGASVCIYCRSRVEHPDVDGLCKLRGKF |
| TP29M (Tat-P29-R93A and F96A) | *YGRKKRRQRRRGSG*YGGASVCIYCRSRVEHPDVDGLCKLAGKA |
| TP29S (Tat-scrambled P29) | *YGRKKRRQRRRGSG*VLKLSCCYDGYIRACSRVGEPVGGSDDFH |

[a] Italics indicate the sequence of HIV-Tat.

requirements throughout the experiments. Intrahepatic (i.h.) inoculations were carried out under anesthesia with 4% chloral hydrate, and all efforts were made to minimize suffering.

**Cell viability, peptide inhibition, and luciferase activity assays.** Cell viability of L2, BHK-21, and Vero E6 cells in 96-well plates was assessed 16 h after peptide was added by cell counting kit 8 (CCK8) (Dojindo). Cell culture in each well was added to 10 μl of CCK8 solution {WST-8 [2-(2-methoxy-4-nitropheny)-3-(4-nitrophenyl)-5-(2,4-disulfophenyl)-2H-tetrazolium, monosodium salt]}, which specifically stained the living cells, by following the manufacturer's protocol.

L2 cells were infected with viruses at a multiplicity of infection (MOI) of 0.1 and incubated at 33°C for 1 h. Infected cells were washed three times with 2 ml of DMEM and supplied with peptide at a final concentration of 200 μM in prewarmed 10% FBS-DMEM. Cells then were incubated at 33°C, and the virus was collected at 20 h postinfection (p.i.). Virus titers were determined by Virus Counter (Virocyt Virus Counter 2100) and plaque assays. For measurement with the Virus Counter, virus in cell culture was collected at room temperature and centrifuged at 14,000 rpm for 10 min, and then the supernatant was added in sample dilution buffer at a 1:10 dilution. Subsequently, in the process of staining, combo dye was mixed with the sample at a ratio of 1:2 and incubated in the dark for 30 min at room temperature. The number of virus particles was determined by following the manufacturer's protocol.

BHK-21 cells were transfected with Rep-SCV-luc/neo reporters (180 ng) together with pRL-TK (50 ng; as transfection efficiency control) with FuGENE HD transfection reagent (Roche Applied Science) according to the manufacturer's instructions. The peptides were added to the culture medium at a final concentration of 200 μM at 1 h posttransfection. The cells were collected and lysed at 20 h posttransfection (32) and then subjected to luciferase activity assays using the Dual-Glo system (Promega, Madison, WI) by following the manufacturer's protocol.

**Viral infection of mice, histological analysis, and alanine aminotransferase (ALT) measurements.** Groups of 3-week-old mice were infected by i.h. inoculation with MHV-A59 diluted in PBS containing 0.75% bovine serum albumin or an equal volume of uninfected cell preparation (mock infection) at a comparable dilution. Liver tissues were harvested at the indicated days postinfection. The tissues were cut into blocks and fixed in phosphate-buffered 4% paraformaldehyde, pH 7.4, for tissue embedding or frozen in PBS with 0.167% gelatin for determining the titers of infectious virus (33).

For the homogenization, livers were soaked in chilled PBS and ground in a tissue homogenizer (OSE-Y20; Tiangen) at 4°C with 20 volumes of PBS. The homogenates were centrifuged for 10 min at 400 × *g* and the supernatant kept at −20°C until use. Standard plaque assays were performed on L2 cells as described previously (34).

For the measurement of the inhibition of peptides on the virus replication in mouse, groups of mice were infected by i.h. inoculation with 500,000 PFU of MHV-A59, and then the peptide (TP29, TP29M, or TP29S), at a final concentration of 0.5 mg/g of body weight, or PBS (nontreatment control) was injected intrahepatically. Mice for each test group were sacrificed at days 1, 3, 5, and 7 postinfection, and the livers were removed and placed directly into 2 ml of isotonic saline with 0.167% gelatin, weighed, and stored frozen at −70°C until use.

For the measurement of ALT/glutamic-pyruvic transaminase (GPT) levels, blood was incubated with serum accelerator at room temperature to allow coagulation and then was centrifuged to obtain serum; the serum was used for measurements of ALT levels using an ALT/GPT kit (C009-2; NJJCBIO).

## RESULTS

**Stimulation of the 2′-O-MTase activity of nsp16 by nsp10 is a common mechanism for coronaviruses.** Previous studies have revealed that FCoV nsp16 alone possesses 2′-*O*-MTase activity but SARS-CoV nsp16 requires the stimulation of nsp10 (25–28). To address this disparity and test whether the nsp10 from other coronaviruses displays stimulatory function, we characterized the 2′-*O*-MTase activity of representative viruses from three coronavirus genera: transmissible gastroenteritis virus (TGEV) and FCoV from *Alphacoronavirus*, mouse hepatitis virus (MHV) from lineage A of *Betacoronavirus*, SARS-CoV from lineage B of *Betacoronavirus*, MERS-CoV from lineage C of *Betacoronavirus*, and infectious bronchitis virus (IBV) from *Gammacoronavirus*. The recombinant nsp10s and nsp16s of these coronaviruses were expressed and purified, and SDS-PAGE analysis showed that the purity of the recombinant proteins was more than 95% with the expected molecular mass (Fig. 1A). As different cloning sites were used, the nsp16 and nsp10 of TGEV, FCoV, and MERS-CoV contain 30 additional amino acid residues at their N termini, leading to slower mobility than that of SARS-CoV, MHV, and IBV (Fig. 1A) but no activity reduction (Fig. 1B to H). The biochemical assays were performed to measure the MTase activity of each nsp16 in the presence or absence of the corresponding nsp10 using cap-0 RNA (m7GpppA-RNA) and $^{3}$H-labeled S-adenosyl-[methyl-$^{3}$H]methionine as substrates. SARS-CoV nsp7 and vaccinia virus VP39, the latter representing a well-characterized 2′-*O*-MTase, were used as negative and positive controls, respectively. As shown in Fig. 1, nsp10 or nsp16 alone of all the coronaviruses, except FCoV nsp16 (Fig. 1C), did not show 2′-*O*-MTase activity. FCoV nsp16 alone showed a low but detectable MTase activity, which is consistent with a previous report (25). In contrast, in the presence of the corresponding nsp10, the nsp16s of TGEV (Fig. 1B), MHV (Fig. 1D), SARS-CoV (Fig. 1E), MERS-CoV (Fig. 1F), and IBV (Fig. 1G) were activated and showed robust MTase activities. Although the nsp16 of FCoV alone could methylate the RNA substrate to a certain extent, its MTase activity was increased more than 3-fold in the presence of nsp10 (Fig. 1C). These results clearly indicate that the stimulation of nsp16 MTase activity by nsp10 is a common mechanism for coronaviruses, including FCoV. To further confirm the position of methylation on the RNA substrates, the cap-0 m7G*pppA-RNA was treated with nsp16 or nsp10/nsp16 complex of all selected coronaviruses. The methylated RNAs were digested with nuclease P1 that cleaves capped RNAs into 3′-OH-terminated cap structures and 5′-p$N_{OH}$. The result-

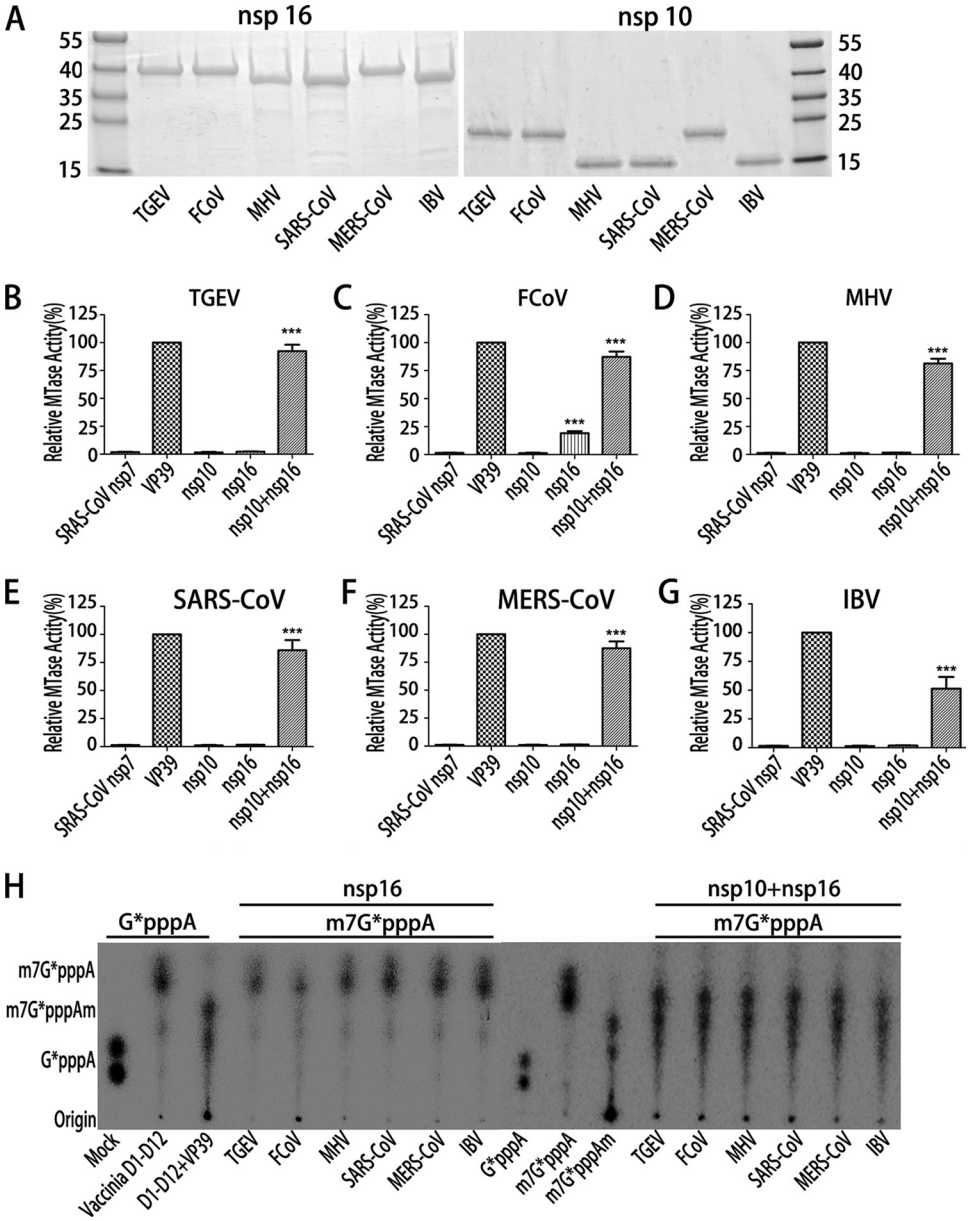


**FIG 1** Biochemical analysis of the 2′-***O***-MTase activity of coronavirus proteins. (A) SDS-PAGE of the recombinant nsp16 and nsp10 of 6 coronaviruses. (B to G) Purified nsp10 (18 μM) and nsp16 (3.0 μM) of the indicated coronaviruses were incubated with the substrate m7GpppA-RNA (with a cap-0 structure at the 5′ end) in the presence of [$^3$H]AdoMet. The 2′-*O*-MTase activities were analyzed by liquid scintillation assays after purification of the $^3$H-labeled substrates with DEAE-Sephadex chromatography. SARS-CoV nsp7 and vaccinia virus 2′-*O*-MTase (VP39) were used as a negative and positive control, respectively ($n = 3$; mean values ± standard deviations [SD]). ***, $P < 0.001$ (unpaired Student's *t* test). (H) TLC analysis of nuclease P1-resistant cap structures released from $^{32}$P-labeled m7G*pppA-RNA methylated by nsp16 or nsp10/nsp16 complex of TGEV, FCoV, MHV, SARS-CoV, MERS-CoV, or IBV. The markers G*pppA, m7G*pppA, and m7G*pppAm were prepared with commercial vaccinia virus capping enzymes. The position of origin and migration of G*pppA, m7G*pppA, and m7G*pppAm are indicated on the left. SARS-CoV nsp7, vaccinia virus N7-MTase (D1 to D12), and 2′-*O*-MTase (VP39) were used as a negative and positive control, respectively.

ing cap structures were analyzed by thin-layer chromatography (TLC). As expected, the P1 cleavage products of RNA treated with nsp10/nsp16 complex comigrated with m7G*pppAm, the cap-1 structure (Fig. 1H). In contrast, the cleavage products treated by nsp16 alone remained as cap-0 structure m7G*pppA, except for FCoV nsp16 treatment, which generated a small fraction of products that comigrated with m7G*pppAm structure (Fig. 1H).

Although structural analysis shows that nsp10 and nsp16 stay at the ratio of 1:1 in the nsp10/nsp16 complex of SARS-CoV (27, 28), nsp10 is translated 3 to 5 times more than nsp16 in the infected cells (35, 36). Therefore, we investigated whether the physiological surplus of nsp10 plays a role in the enzymatic activity of nsp16, especially for FCoV nsp16. As shown in Fig. 2, nsp10 could significantly increase the enzymatic activity of coronavirus nsp16 in a dose-dependent manner, including FCoV nsp16. The ratio of nsp16 to nsp10 for maximal enzymatic activity of FCoV 2′-*O*-

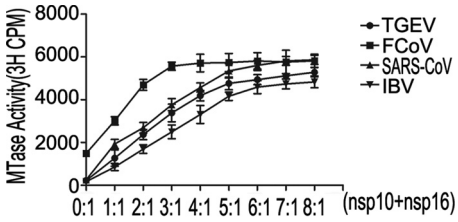


**FIG 2** MTase assays of coronavirus nsp16 with different molar ratios of cognate nsp10. The substrate $m^7$GpppA-RNAs with a cap-0 structure were used to test the 2′-*O*-MTase activities of nsp16 of TGEV, FCoV, SARS-CoV, and IBV. The ratio of nsp10 to nsp16 is indicated below the *x* axis ($n = 3$; mean values ± SD).

MTase is 1:3, while it is around 1:8 for other coronaviruses, although the MTase activities did not significantly increase from 1:6. This is consistent with the physiological ratio of nsp16 to nsp10 in infected cells. Therefore, the ratio 1:6 of nsp16 to nsp10 was used in the following biochemical assays to mimic the physiological environment of coronaviral infection.

**The nsp10s of coronaviruses are interchangeable in stimulating the nsp16 2′-*O*-MTase activity among coronaviruses.** In previous studies, the crystal structure of SARS-CoV 2′-*O*-MTase revealed the critical residues involved in the interaction between nsp10 and nsp16 which might contribute to the binding of cofactor SAM (such as Lys93 of nsp10 with Ser105 of nsp16) (28) and RNA substrates (such as Tyr96 of nsp10 with Gln87, Arg86, Ala83, and Val84 of nsp16) (27, 28, 37). Although alignments of primary sequences of both nsp10 (Fig. 3A) and nsp16 (Fig. 3B) of coronaviruses showed similarity of approximately 40%, the identified critical residues on the interaction interface of nsp10 and nsp16 of SARS-CoV are highly conserved among coronaviruses (Fig. 3A and B). Therefore, we assumed that the nsp10 of one coronavirus is able to stimulate the nsp16 2′-*O*-MTase of another virus. To test this assumption, we first analyzed whether nsp10 was interchangeable among the coronaviruses of the same genus. As shown in Fig. 3C and D, the MTase activities of nsp16 could be stimulated efficiently by any other nsp10 from the same genus to a similar level. We further analyzed the stimulatory effect of nsp10 from coronaviruses of different genera. As shown in Fig. 4, the nsp16 of TGEV could be fully stimulated by the nsp10 of *Alphacoronavirus* and less efficiently activated when using the nsp10 of *Betacoronavirus* and *Gammacoronavirus* (Fig. 4A). In contrast, the FCoV nsp16 could be stimulated to a similar level either by cognate nsp10 or noncognate nsp10s (Fig. 4B), which may reflect the fact that FCoV nsp16 alone already possesses a certain degree of MTase activity (Fig. 1C), indicating that it is further stimulated more efficiently by an nsp10 of any coronavirus. Interestingly, nsp16s of *Betacoronavirus*, including MHV (Fig. 4C), SARS-CoV (Fig. 4D), and MERS-CoV (Fig. 4E), could be fully activated and stimulated with the help of nsp10s of all selected coronaviruses from different genera. In contrast, the nsp16 of IBV (*Gammacoronavirus*) was activated and stimulated remarkably only by its cognate nsp10 (Fig. 4F). Taken together, these results indicate that the characteristics of coronavirus nsp10 and nsp16 vary, but the mechanisms of 2′-*O*-MTases stimulated by nsp10s are relatively conserved. Moreover, the nsp10s of different coronaviruses may share some critical residues for binding nsp16s, and they are functionally interchangeable among different coronaviruses.

**Development of a broad-spectrum peptide inhibitor against coronaviral 2′-*O*-MTase.** The conserved mechanism and interchangeability of nsp10 in the activation and stimulation of coronaviral 2′-*O*-MTases provides the possibility to develop broad-spectrum inhibitors for repressing the 2′-*O*-MTase activities of different coronaviruses. In previous studies, we showed that the region of aa 65 to 107 of nsp10 is sufficient for the interaction with nsp16 but unable to stimulate the 2′-*O*-MTase activity, while peptides derived from this region could suppress nsp16 activity *in vitro* (30). In this study, we designed a peptide that corresponds to aa 68 to 96 of MHV nsp10 and tested its inhibitory effects in the replication models of MHV and SARS-CoV replicons. Two residues (the basic K93 and aromatic Y96) of SARS-CoV nsp10 were shown to be critically involved in the interaction with nsp16 (27, 28, 37) and are well conserved in nsp10 of different coronaviruses, where the lysine can be replaced by arginine (R) and tyrosine by phenylalanine (F) (Fig. 3A, marked by open triangles). To confirm that these two residues are important for the stimulatory function of nsp10, recombinant nsp10s of 6 coronaviruses with either K/R-to-A or Y/F-to-A mutation were expressed, purified, and tested in MTase activity assays. As shown in Fig. 5A, when either of the two critical residues was changed to alanine, the stimulatory function of nsp10 was largely disrupted, indicating that the two residues are essential for stimulating nsp16 activity. To test the inhibitory effect of MHV nsp10-derived peptide on nsp16 of different coronaviruses, we chemically synthesized three peptides: P29 (aa 68 to 96 of MHV), P29M (P29 sequence with mutations of the critical residues, R93A and F96A), and P29S (with scrambled sequence of P29) (Table 1). P29M and P29S were used as negative controls in the assays. The peptides were added to the mixture of nsp16s and nsp10s in the MTase assays. As shown in Fig. 5B, compared to P29M and scrambled peptide P29S, P29 could significantly inhibit the MTase activity of nsp16s of MHV, SARS-CoV, MERS-CoV, and IBV by more than 50% inhibitory efficiency and modestly repress that of nsp16s of *Alphacoronavirus* (TGEV and FCoV). These results indicate that the peptide P29 derived from the interaction domain of MHV nsp10 possesses a broad-spectrum inhibitory activity on nsp10/nsp16 complex of a number of different coronaviruses in the *in vitro* assays.

**Inhibition of coronavirus replication by P29 in cell culture models.** We next tested whether the peptide P29 could inhibit virus replication in the replication models of MHV live virus and SARS-CoV replicon. To deliver the short peptide to cells, the N terminus of peptides P29, P29M, and P29S was fused with a short peptide from HIV-Tat (YGRKKRRQRRRGSG), which is arginine rich and can act as a cell-penetrating carrier to deliver the cargo to the cytosol and nucleus (38). The HIV-Tat fused peptides were named TP29, TP29M, and TP29S, respectively (Table 1). To evaluate the cytotoxicity of the Tat fused peptides, cell viability was tested by CCK8 assays, which showed that they were well tolerated by baby hamster kidney cells (BHK-21), Vero E6 cells, and rat lung epithelial cells (L2) at final concentrations of 20 to ~400 μM, and no cytotoxicity was observed (data not shown).

We first tested the inhibitory effects of P29 on MHV replication. L2 cells were infected with MHV-A59 at a multiplicity of infection (MOI) of 1. One hour after infection, peptides TP29, TP29M, P29, and TP29S were added to the culture medium at a final concentration of 200 μM. Virus titers were measured (Fig. 6A) and further verified by plaque assays (Fig. 6B) 20 h postinfection. TP29 reduced the titer of MHV-A59 by 80% compared to that of the

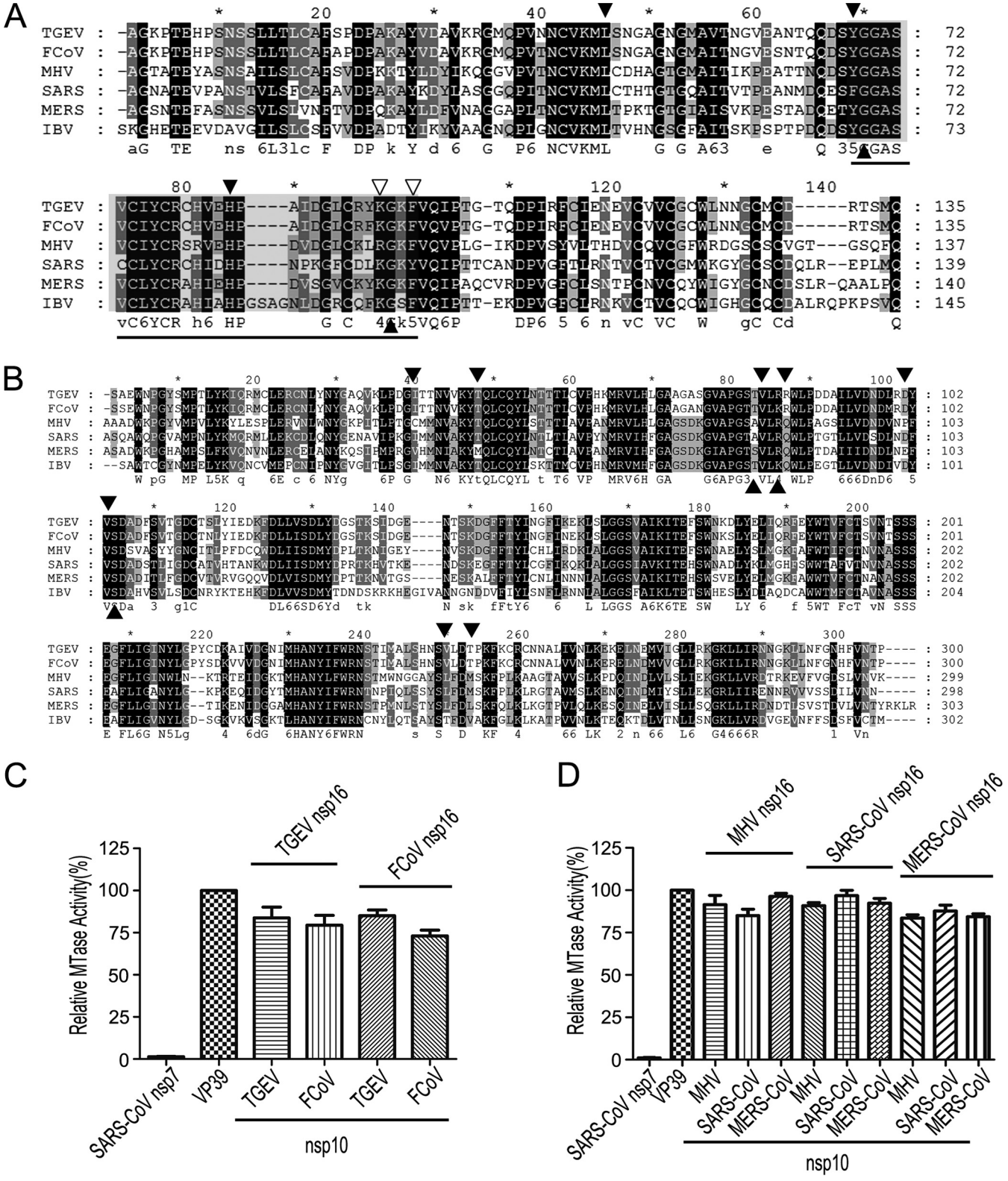


**FIG 3** Conservation of nsp10 and nsp16 in coronaviruses. (A and B) Primary sequence alignments of nsp10 (A) and nsp16 (B) of TGEV, FCoV, MHV, SARS-CoV, MERS-CoV, and IBV. The well-conserved and relatively conserved residues are indicated by solid black boxes and solid gray boxes, respectively. The conserved residues involved in the interactions of nsp10/nsp16 complexes are indicated by solid black and open triangles. The region corresponding to the peptide inhibitor P29 is marked by a line. The alignment was generated with the program Clustal, and the figure was prepared using Genedoc. (C and D) MTase assays of alphacoronaviral nsp16 (C) and betacoronaviral nsp16 (D) stimulated by the noncognate nsp10 from a coronavirus of the same genus. SARS-CoV nsp7 and vaccinia virus 2′-*O*-MTase (VP39) were used as a negative and positive control, respectively ($n = 3$; mean values ± SD).

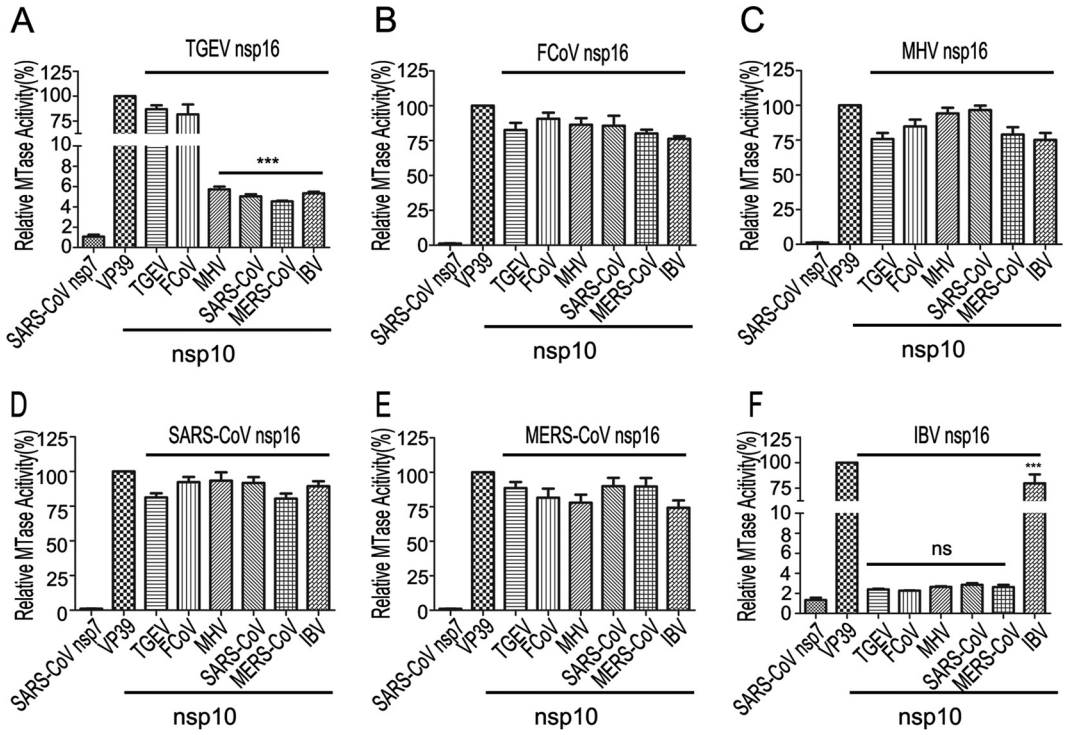


**FIG 4** MTase assays of nsp16 stimulated by noncognate nsp10 from different genera of coronaviruses. The m7GpppA-RNAs with a cap-0 structure were used to test the 2′-*O*-MTase activities of nsp16 of TGEV (A), FCoV (B), MHV (C), SARS-CoV (D), MERS-CoV (E), and IBV (F) stimulated by nsp10 from different genera of coronaviruses as indicated. SARS-CoV nsp7 and vaccinia virus 2′-*O*-MTase (VP39) were used as a negative and positive control, respectively ($n = 3$; mean values ± SD). ***, $P < 0.001$; ns, not significant (unpaired Student's *t* test).

mock control (PBS), while TP29M, TP29S, and P29 did not display significant inhibitory effects (Fig. 6A and B). Notably, the peptide P29 showed inhibitory activity in the *in vitro* assays (Fig. 5B) but not in cell cultures, indicating that the fused HIV-Tat peptide is essential for the delivery of the peptides into cells. Moreover, the average diameter of viral plaque with TP29 treatment was two times smaller than that with TP29S 20 h postinfection (Fig. 6C), which indicates that TP29 slowed down the growth of MHV-A59. The dose-response curve of TP29 showed that the 50% inhibitory concentration ($IC_{50}$) against MHV is approximately 60 μM (Fig. 6D).

We then tested the capacity of the peptides TP29, TP29M, and TP29S to inhibit the replication of SARS-CoV replicon (Rep-SCV-luc/neo), which harbors the firefly luciferase reporter gene under the control of M gene transcription regulatory sequence (TRS) (32). Renilla luciferase was employed as a transfection control. The peptides were added to the culture medium at a final concentration of 200 μM, 1 h after cotransfection of Rep-SCV-luc/neo and Renilla luciferase in BHK-21 cells. As shown in Fig. 6E, compared with TP29M and TP29S, TP29 repressed the replication of the SARS-CoV replicon by 50%. Together, these results suggest that peptide TP29 could suppress the replication of different coronaviruses in cell cultures, consistent with its broad-spectrum activity observed in the *in vitro* assays.

**Peptide TP29 can rescue MHV-infected mice by inhibiting viral replication and enhancing the IFN response.** We further tested whether peptide TP29 could inhibit virus replication *in vivo* in an animal model. C57BL/6 mice ($n = 10$) were infected by intrahepatic (i.h.) inoculation with 500,000 PFU of wild-type

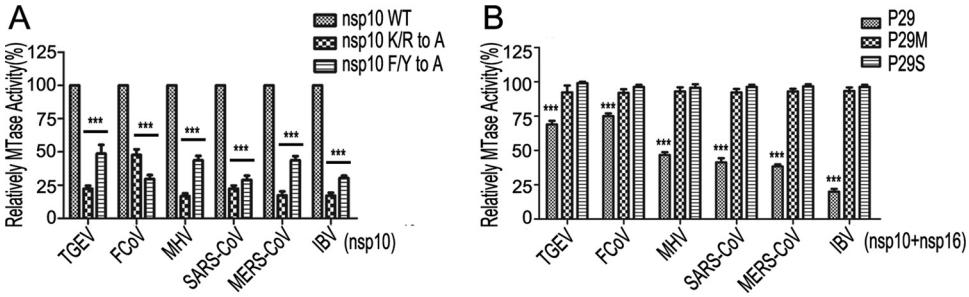


**FIG 5** Biochemical analyses of nsp10 mutants and its derived short peptides. (A) The MTase activities of nsp16 of TGEV, FCoV, MHV, SARS-CoV, MERS-CoV, and IBV, stimulated by corresponding wild-type nsp10 and their mutant, K/R to A or F/Y to A, were tested by MTase assays. (B) The inhibition effects of P29, P29M, and P29S peptides at a final concentration of 200 μM on 2′-*O*-MTase activities of different coronaviruses ($n = 3$; mean values ± SD). ***, $P < 0.001$ (unpaired Student's *t* test).

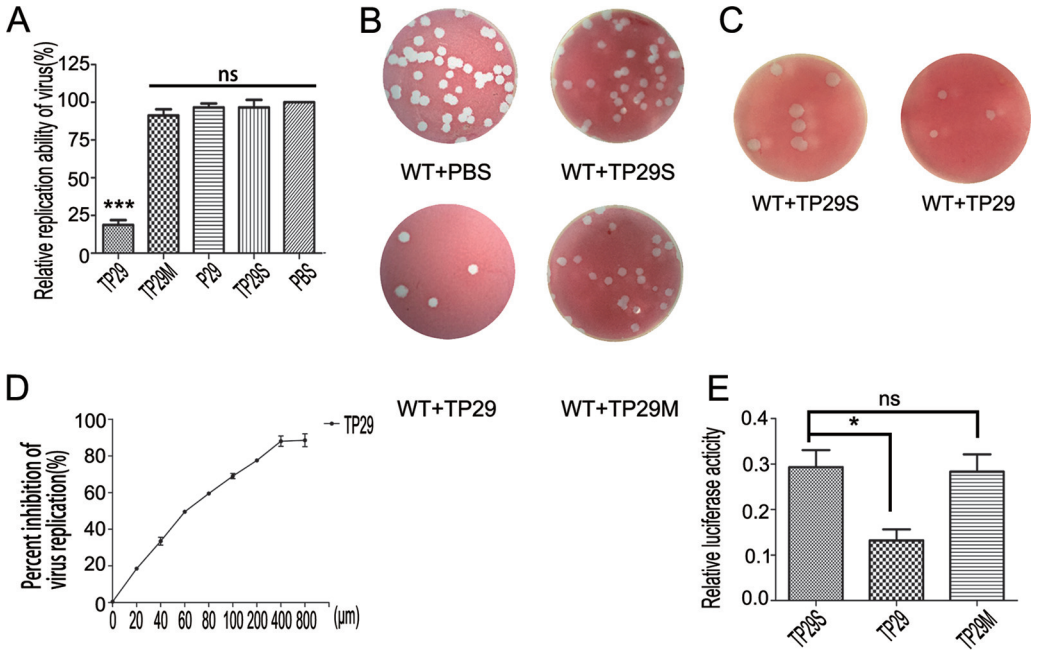


**FIG 6** Inhibitory effects of short peptides on coronavirus replication in cell culture models. (A and B) The inhibitory effects of the peptides TP29, TP29M, P29, and TP29S at a final concentration of 200 μM and PBS control on the replication of MHV-A59 in L2 cells. The virus titers were determined by virus counter (A) and further confirmed by the plaque assays in L2 cells 20 h postinfection (B). (C) The plaque size of MHV-A59 on L2 cells with treatment of TP29S or TP29 at a final concentration of 200 μM. (D) Inhibition effects of TP29 at different final concentrations (0 to 800 μM) on the replication of MHV-A59. (E) The inhibitory effects of the indicated peptides on the replication of SARS-CoV replicon ($n = 3$; mean values ± SD). *, $P < 0.05$; **, $P < 0.01$; ***, $P < 0.001$; ns, not significant (unpaired Student's *t* test).

MHV-A59 or an equal volume of uninfected cell preparation (mock infection) at a comparable dilution. The peptides (TP29 or TP29S) at a final concentration of 0.05 mg/g or PBS each were intrahepatically injected immediately postinfection of MHV-A59. The survival percentage of each group (mock infection and MHV infection with TP29, TP29S, and PBS) was statistically analyzed during the 14-day observation period (Fig. 7A). The MHV-infected mice supplied with TP29S and PBS began to die at day 4 p.i., and all of them (10/10) died by 7 days postinfection (Fig. 7A). However, all (10/10) of the infected mice treated by TP29 and the mice inoculated with uninfected cell preparation (mock infection) survived (Fig. 7A), which exceeds expectations considering its inhibitory effect in cell culture models (Fig. 6). To evaluate the effects of TP29 on virus replication and pathological changes, C57BL/6 mice ($n = 7$) were infected with MHV-A59 as described above and intrahepatically injected with peptides or PBS (mock control) immediately (0 h) or 1 h postinfection. The mice were sacrificed at day 3 postinfection, and viral titers in livers (Fig. 7B) and serum alanine aminotransferase (ALT) values (Fig. 7C) of each group were analyzed. Interestingly, with the protection of TP29 at or after infection, the virus titers of MHV-infected mouse livers sharply decreased by 1.5 $\log_{10}$ (Fig. 7B), and the serum ALT values, which indicate the damage level of liver cells caused by the virus-induced acute hepatitis in clinical diagnosis (39), were 10 times less than that of other groups (Fig. 7C). Moreover, the intrahepatic injection of the peptides showed no side effects to hosts as the ALT values in mock infection controls remained at background levels (Fig. 7C). These results demonstrated that the inhibitory efficacy of TP29 *in vivo* is significantly higher than that in cell cultures (Fig. 6), which implies that an additional antiviral mechanism, such as innate immunity, is enhanced besides the direct inhibitory effect of TP29 on the nsp16 MTase activity.

The nsp16 2′-*O*-MTase activity has been shown to play an important role in the evasion of innate immunity, and deficiency in the 2′-*O*-MTase may lead to increased IFN responses against virus infection (6, 7). Therefore, we further tested whether TP29 treatment could increase IFN production during MHV infection and analyzed IFN-β levels as well as serum ALT values in the MHV-infected C57BL/6 mice ($n = 7$) treated by TP29, TP29S (scrambled TP29), or PBS. In addition, one group of mice was treated with TP29 but not infected with MHV. The mice were sacrificed 1, 3, 5, and 7 days postinfection. As shown in Fig. 7D and E, the serum IFN-β levels of TP29-treated mice were significantly enhanced 24 h postinfection, while the virus titer was 1.5 $\log_{10}$ times lower than that in TP29S-treated mice (Fig. 7D). The treatment with TP29 without MHV infection did not enhance IFN-β production in mice (Fig. 7D). In contrast, the serum IFN-β levels of TP29S-treated mice sharply increased to 115 pg/ml 72 h (3 days) postinfection (Fig. 7D). Accordingly, the viral titers of TP29S-treated mice kept increasing and finally were killed 6 days postinfection (Fig. 7E). The kinetics of serum ALT values showed that the livers of TP29-treated mice were well protected at day 3 postinfection, and the ALT values began to decrease 7 days postinfection (Fig. 7F). These phenomena also were verified by pathological section analysis of mice livers stained with hematoxylin and eosin. As shown in Fig. 7G, the number and size of the foci of hepatocyte necrosis, inflammatory cells, and lymphocytic infiltration, which represent acute hepatitis in the liver parenchyma, were significantly smaller in TP29-treated mice than in other groups; the liver of the former was restored to a normal state 7 days postinfection. Taken together, these results indicate that the peptide TP29 could rescue MHV-infected mice by inhibiting viral replication and inducing the IFN response at an early stage of infection. Therefore, the increase of IFN response by TP29 treatment may

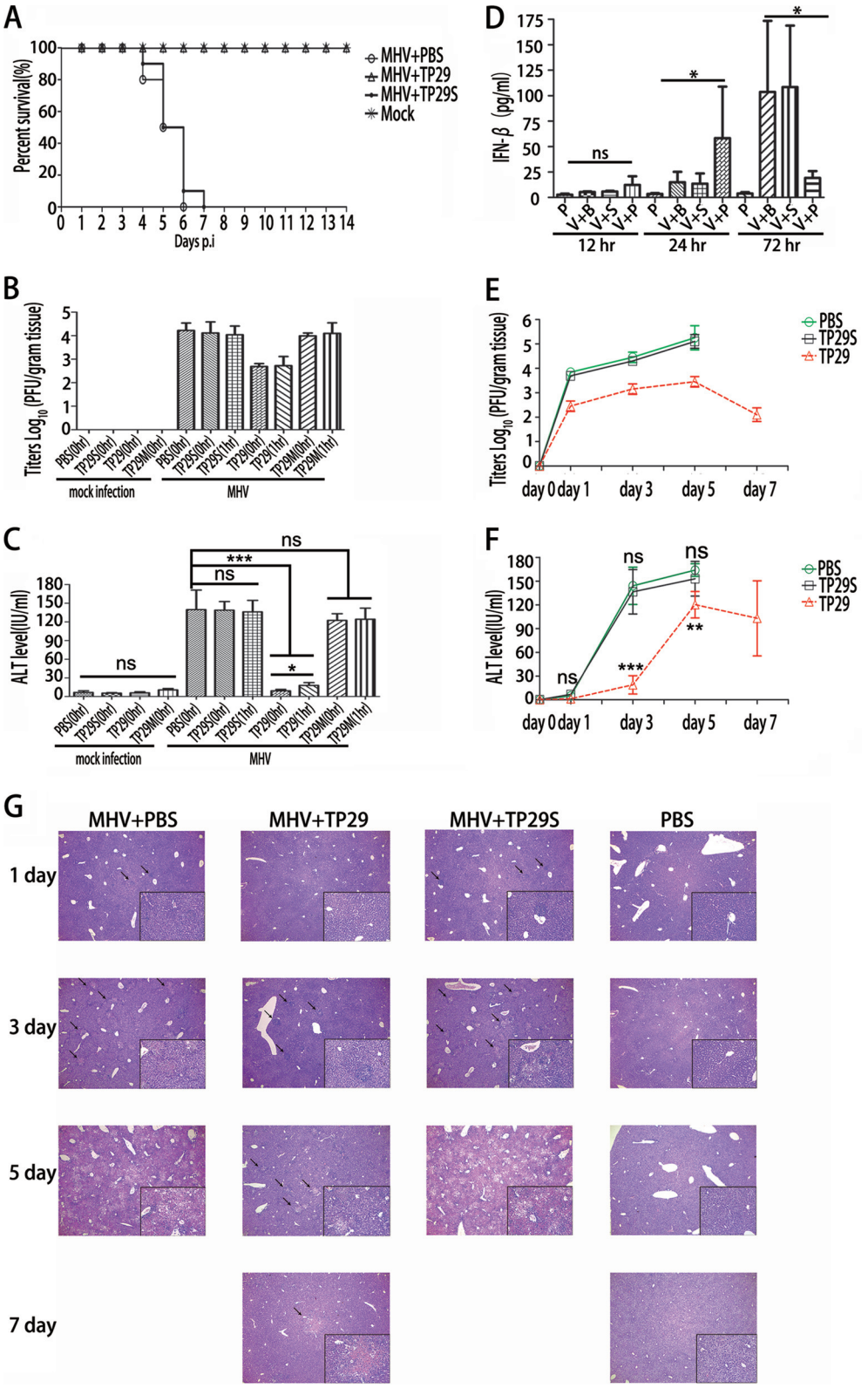


**FIG 7** Rescue of MHV-infected mice by peptide inhibitor TP29. (A) Lethality of groups of MHV-infected or mock-treated mice ($n = 10$) after treatment with peptides (PBS, TP29, and TP29S). The mice were monitored for 14 days. (B and C) Viral titers of clarified liver homogenates (B) and serum ALT (alanine aminotransferase) values (C) were determined at day 3 postinfection. Zero hour or 1 h represents that peptides were injected immediately or 1 h after the mice ($n = 7$) were infected with MHV-A59. The virus titer was normalized for liver mass. (D) Enzyme-linked immunosorbent assay of IFN-β in serum 12 h, 24 h, and 72 h postinfection with MHV-A59 and injection of 0.05 mg/g (amount of peptide to body weight of mice) TP29 or TP29S peptide ($n = 7$). V represents MHV infection; B, PBS; P, TP29; S, TP29S (scrambled TP29). TP29 injection without MHV infection (P) was used as a mock control. Viral titers (E) and serum ALT values (F) were measured at the indicated time points. Groups of mice ($n = 7$) were sacrificed at 1, 3, 5, and 7 days p.i. (G) Hematoxylin and eosin staining of paraformaldehyde-fixed liver sections at day 1, 3, 5, and 7 p.i. of C57BL/6 mice (magnification, ×40; inset, ×200) ($n = 7$; mean values ± SD).*, $P < 0.05$; **, $P < 0.01$; ***, $P < 0.001$; ns, not significant (unpaired Student's *t* test).

have contributed to the potent inhibition of virus replication and pathogenesis of MHV infection.

## DISCUSSION

Coronaviruses belong to the largest RNA viruses and form a complicated replication/transcription complex (RTC), which is composed of 16 nonstructural proteins (nsps) and some unknown host factors (40, 41). A number of nsps have been identified as RNA processing/modification enzymes, among which nsp14 is an exoribonuclease/N7-(guanine)-methyltransferase (21–23) and nsp16 is a 2′-*O*-MTase (25–28). In previous studies, it has been shown that SARS-CoV nsp16 exerts the 2′-*O*-MTase activity only in the presence of nsp10, whereas FCoV nsp16 alone possesses the 2′-*O*-MTase activity to some degree (25–28). In this study, we demonstrated that stimulation of the nsp16 2′-*O*-MTase by nsp10 is universal to coronaviruses, including FCoV (Fig. 1 and 4). In contrast to the nsp16 of other coronaviruses, FCoV nsp16 possesses a low but detectable 2′-*O*-MTase activity but is stimulated to full activity by its cognate nsp10 (Fig. 1).

Interestingly, the nsp10s of coronaviruses could activate and stimulate, to various degrees, the 2′-*O*-MTase activities of noncognate nsp16s except that of IBV (*Gammacoronavirus*) (Fig. 4), indicating that both nsp10 and nsp16 have been structurally and functionally conserved during coronavirus evolution. Moreover, the strength of the nsp16 2′-*O*-MTase activity stimulated by noncognate nsp10 corresponds to the phylogenetic distances and taxonomic positions of nsp10 and nsp16 in their phylogenetic trees, in which *Alphacoronavirus* is more closely related to *Betacoronavirus* (data not shown). However, in the phylogenetic tree inferred using genome RNA, *Gammacoronavirus* is more closely related to *Betacoronavirus*, indicating that nsp10 has coevolved with nsp16 at the protein level. Furthermore, the nsp10 mutants of IBV (K to A and F to A; indicated by open triangles in Fig. 3A) showed the weakest stimulation capability of 2′-*O*-MTase among the other coronaviruses studied (Fig. 5A). These results indicate that the stimulation of IBV (gammacoronaviral) 2′-*O*-MTase activity most strictly depends on the assistance of its cognate nsp10, and the two critical residues of IBV nsp10 are essential for the interaction of the nsp10/nsp16 complex. Therefore, although MHV nsp10 cannot stimulate IBV nsp16, the interaction domain of MHV nsp10 that contains the two critical residues and is 4 amino acids shorter than the corresponding interaction region of IBV nsp10 (Fig. 3A) still could possess the capability to bind with nsp16 of IBV. Such an assumption was supported by our result that the peptide P29 that is derived from the interaction domain of MHV nsp10 could strongly suppress the 2′-*O*-MTase activity of IBV (Fig. 5B). The conserved mechanism and the interchangeability of nsp10 in stimulating nsp16 provide a theoretical basis for possible development of broad-spectrum inhibitors by targeting coronaviral nsp10/nsp16 2′-*O*-MTase (Fig. 6).

During coronavirus replication, ORF1b (harboring nsp16) is translated via a −1 ribosomal frameshifting mechanism from ORF1a that contains nsp10 (42), and consequently nsp10 is produced in a 3- to 5-fold excess relative to the level of nsp16 in infected cells (35, 36). Although nsp10 and nsp16 exist at a 1:1 ratio in the crystal structure (27, 28), we demonstrate that the surplus nsp10 could significantly increase the enzymatic activity of nsp16 (Fig. 2). Moreover, the critical residues of nsp10s (K/R and F/Y; indicated by open triangles in Fig. 3A), which are essential for the stimulation of 2′-*O*-MTase activities of coronaviruses (Fig. 5A), are concentrated in the interaction region of around 42 amino acids. In contrast, the conserved residues of nsp16s involved in the interaction of the nsp10/nsp16 complex are scattered throughout a large region of the protein and brought together to the interface by protein folding (28, 30). Therefore, it is more feasible to design inhibitory peptides by mimicking the sequence of the interaction interface of nsp10 rather than that of nsp16. Compared with the MTase inhibitors previously used in research work, the peptide inhibitor developed based on the characteristics of coronavirus 2′-*O*-MTases could more specifically repress viral replication with fewer side effects (Fig. 6 and 7) because it specifically targets the viral structure that does not exist in cellular proteins.

Previous studies have revealed that the viral RNA cap structures play important roles in viral replication, evasion of recognition by host RNA sensors, and suppression of IFN-mediated antiviral response (6, 7). Therefore, antiviral drugs targeting the viral RNA capping enzymes may lead to both inhibition of virus replication and enhancement of interferon responses, as we demonstrated in this study (Fig. 7). It is interesting that the inhibitory efficiency of TP29 was remarkably higher *in vivo* in animal infection than that in biochemical assays and cell culture. This may be explained by the enhancement of antiviral response *in vivo* when the 2′-*O*-MTase activity is inhibited by the peptide. Many studies have reported that coronaviruses are poor inducers of type I IFN in cell lines (43). However, in primary cells such as plasmacytoid dendritic cells (pDC) and macrophages, IFN is induced by MHV infection (33, 44, 45). In this study, we assume that TP29 treatment suppressed the 2′-*O*-MTase activity of nsp10/nsp16, which may lead to an increase of the blood level of IFN-β at the early stage of infection and consequently enhance the antiviral immunity in animals. Here, we propose a testable hypothesis to explain how the peptide inhibitor promotes antiviral response and suppresses virus replication (Fig. 8). First, the peptide may inhibit the formation of nsp10/nsp16 complex and the 2′-*O*-MTase activity, directly contributing to the suppression of genome replication; second, the reduced 2′-*O*-MTase activity of nsp16 may lead to deficiency in the 2′-*O*-methylation in the RNA cap structure, resulting in more cap-0 structures, which have a lower efficiency of translation and consequently suppress the synthesis of viral proteins; and third, the viral RNA lacking a cap-1 structure can be recognized by innate RNA sensors and stimulate the type I interferon responses (Fig. 8). These possibilities shall be tested in future studies to reveal the mechanisms of peptide-mediated inhibition of coronavirus replication.

In conclusion, our data demonstrate that stimulation of nsp16 2′-*O*-MTase activity by nsp10 is a common mechanism for coronaviruses, and nsp10 is functionally interchangeable in activation and stimulation of noncognate nsp16 among different coronaviruses. Moreover, broad-spectrum inhibitors can be developed by targeting the nsp10/nsp16 2′-*O*-MTase, as demonstrated by the result that the MHV nsp10-derived TP29 peptide can suppress 2′-*O*-MTase activity of different coronaviruses and efficiently suppress MHV-induced pathogenesis in mice by promoting antiviral responses. Therefore, our study provides experimental evidence and proof of principle that a peptide inhibitor targeting the 2′-*O*-MTase can efficiently suppress coronavirus replication, suggesting that the 2′-*O*-MTases of coronaviruses are ideal and potential antiviral drug targets. In future work, more potent peptides will be screened and optimized to inhibit the 2′-*O*-MTase activity and replication of coronaviruses.

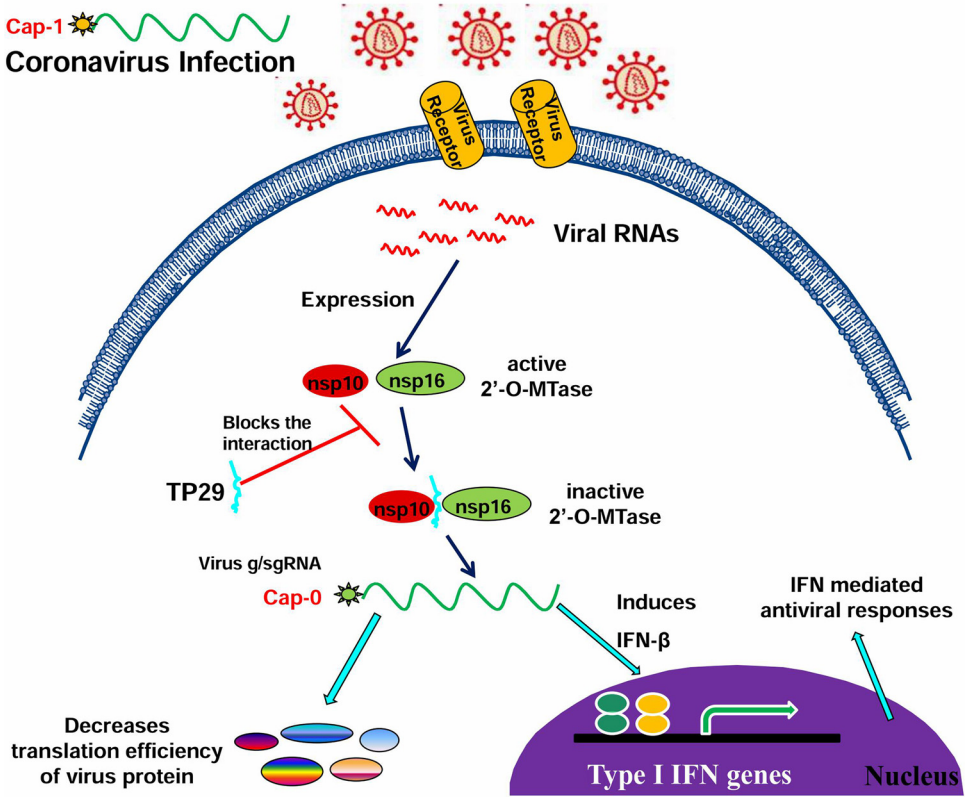


**FIG 8** Hypothesis for the mechanisms of peptide TP29-mediated inhibition of coronavirus infection. Peptide inhibitor TP29 may modulate three steps in the coronavirus replication cycle: inhibiting the formation of nsp10/nsp16 complex, decreasing the translation efficiency of viral RNAs, and promoting the recognition of viral RNAs by cellular innate RNA sensors, leading to enhanced immune responses.

## ACKNOWLEDGMENTS

We thank Eric J. Snijder for kindly providing the expression plasmids for IBV nsp16 and nsp10 (pDest14-IBV-nsp16 and pDest14-IBV-nsp10), Peter J. M. Rottier for the FCoV cDNA, and Rong Ye for MHV strain A59 and L2 cells. We are grateful to Luis Enjuanes for providing the TGEV cDNA and SARS-CoV replicon.

This research was supported by the China "973" Basic Research Program (2013CB911101), China NSFC grants (81130083, 81271817, 31170152, and 31221061), the Wuhan Science and Technology Project (2014060101010055), and the Sigrid Juselius Foundation.

## REFERENCES

1. **Furuichi Y, Shatkin AJ.** 2000. Viral and cellular mRNA capping: past and prospects. Adv Virus Res **55:**135–184.
2. **Liu H, Kiledjian M.** 2006. Decapping the message: a beginning or an end. Biochem Soc Trans **34:**35–38. http://dx.doi.org/10.1042/BST0340035.
3. **Pichlmair A, Schulz O, Tan CP, Naslund TI, Liljestrom P, Weber F, Reis e Sousa C.** 2006. RIG-I-mediated antiviral responses to single-stranded RNA bearing 5′-phosphates. Science **314:**997–1001. http://dx.doi.org/10.1126/science.1132998.
4. **Hornung V, Ellegast J, Kim S, Brzozka K, Jung A, Kato H, Poeck H, Akira S, Conzelmann KK, Schlee M, Endres S, Hartmann G.** 2006. 5′-Triphosphate RNA is the ligand for RIG-I. Science **314:**994–997. http://dx.doi.org/10.1126/science.1132505.
5. **Ray D, Shah A, Tilgner M, Guo Y, Zhao Y, Dong H, Deas TS, Zhou Y, Li H, Shi PY.** 2006. West Nile virus 5′-cap structure is formed by sequential guanine N-7 and ribose 2′-O methylations by nonstructural protein 5. J Virol **80:**8362–8370. http://dx.doi.org/10.1128/JVI.00814-06.
6. **Zust R, Cervantes-Barragan L, Habjan M, Maier R, Neuman BW, Ziebuhr J, Szretter KJ, Baker SC, Barchet W, Diamond MS, Siddell SG, Ludewig B, Thiel V.** 2011. Ribose 2′-O-methylation provides a molecular signature for the distinction of self and non-self mRNA dependent on the RNA sensor Mda5. Nat Immunol **12:**137–143. http://dx.doi.org/10.1038/ni.1979.
7. **Daffis S, Szretter KJ, Schriewer J, Li J, Youn S, Errett J, Lin TY, Schneller S, Zust R, Dong H, Thiel V, Sen GC, Fensterl V, Klimstra WB, Pierson TC, Buller RM, Gale M, Jr, Shi PY, Diamond MS.** 2010. 2′-O methylation of the viral mRNA cap evades host restriction by IFIT family members. Nature **468:**452–456. http://dx.doi.org/10.1038/nature09489.
8. **Woyciniuk P, Linder M, Scholtissek C.** 1995. The methyltransferase inhibitor neplanocin A interferes with influenza virus replication by a mechanism different from that of 3-deazaadenosine. Virus Res **35:**91–99. http://dx.doi.org/10.1016/0168-1702(94)00085-Q.
9. **Chrebet GL, Wisniewski D, Perkins AL, Deng Q, Kurtz MB, Marcy A, Parent SA.** 2005. Cell-based assays to detect inhibitors of fungal mRNA capping enzymes and characterization of sinefungin as a cap methyltransferase inhibitor. J Biomol Screen **10:**355–364. http://dx.doi.org/10.1177/1087057104273333.
10. **Masters PS.** 2006. The molecular biology of coronaviruses. Adv Virus Res **66:**193–292.
11. **Li W, Shi Z, Yu M, Ren W, Smith C, Epstein JH, Wang H, Crameri G, Hu Z, Zhang H, Zhang J, McEachern J, Field H, Daszak P, Eaton BT, Zhang S, Wang LF.** 2005. Bats are natural reservoirs of SARS-like coronaviruses. Science **310:**676–679. http://dx.doi.org/10.1126/science.1118391.
12. **Lau SK, Woo PC, Li KS, Huang Y, Tsoi HW, Wong BH, Wong SS, Leung SY, Chan KH, Yuen KY.** 2005. Severe acute respiratory syndrome coronavirus-like virus in Chinese horseshoe bats. Proc Natl Acad Sci U S A **102:**14040–14045. http://dx.doi.org/10.1073/pnas.0506735102.
13. **Ge XY, Li JL, Yang XL, Chmura AA, Zhu G, Epstein JH, Mazet JK, Hu B, Zhang W, Peng C, Zhang YJ, Luo CM, Tan B, Wang N, Zhu Y, Crameri G, Zhang SY, Wang LF, Daszak P, Shi ZL.** 2013. Isolation and characterization of a bat SARS-like coronavirus that uses the ACE2 receptor. Nature **503:**535–538. http://dx.doi.org/10.1038/nature12711.
14. **Martina BE, Haagmans BL, Kuiken T, Fouchier RA, Rimmelzwaan GF, Van Amerongen G, Peiris JS, Lim W, Osterhaus AD.** 2003. Virology:

SARS virus infection of cats and ferrets. Nature **425:**915. http://dx.doi.org/10.1038/425915a.

15. **de Groot RJ, Baker SC, Baric RS, Brown CS, Drosten C, Enjuanes L, Fouchier RA, Galiano M, Gorbalenya AE, Memish ZA, Perlman S, Poon LL, Snijder EJ, Stephens GM, Woo PC, Zaki AM, Zambon M, Ziebuhr J.** 2013. Middle East respiratory syndrome coronavirus (MERS-CoV): announcement of the Coronavirus Study Group. J Virol **87:**7790–7792. http://dx.doi.org/10.1128/JVI.01244-13.
16. **Gorbalenya AE, Snijder EJ, Spaan WJ.** 2004. Severe acute respiratory syndrome coronavirus phylogeny: toward consensus. J Virol **78:**7863–7866. http://dx.doi.org/10.1128/JVI.78.15.7863-7866.2004.
17. **Brierley I, Digard P, Inglis SC.** 1989. Characterization of an efficient coronavirus ribosomal frameshifting signal: requirement for an RNA pseudoknot. Cell **57:**537–547. http://dx.doi.org/10.1016/0092-8674(89)90124-4.
18. **te Velthuis AJ, Arnold JJ, Cameron CE, van den Worm SH, Snijder EJ.** 2010. The RNA polymerase activity of SARS-coronavirus nsp12 is primer dependent. Nucleic Acids Res **38:**203–214. http://dx.doi.org/10.1093/nar/gkp904.
19. **Imbert I, Guillemot JC, Bourhis JM, Bussetta C, Coutard B, Egloff MP, Ferron F, Gorbalenya AE, Canard B.** 2006. A second, non-canonical RNA-dependent RNA polymerase in SARS coronavirus. EMBO J **25:**4933–4942. http://dx.doi.org/10.1038/sj.emboj.7601368.
20. **Ivanov KA, Thiel V, Dobbe JC, van der Meer Y, Snijder EJ, Ziebuhr J.** 2004. Multiple enzymatic activities associated with severe acute respiratory syndrome coronavirus helicase. J Virol **78:**5619–5632. http://dx.doi.org/10.1128/JVI.78.11.5619-5632.2004.
21. **Minskaia E, Hertzig T, Gorbalenya AE, Campanacci V, Cambillau C, Canard B, Ziebuhr J.** 2006. Discovery of an RNA virus 3′->5′ exoribonuclease that is critically involved in coronavirus RNA synthesis. Proc Natl Acad Sci U S A **103:**5108–5113. http://dx.doi.org/10.1073/pnas.0508200103.
22. **Chen P, Jiang M, Hu T, Liu Q, Chen XS, Guo D.** 2007. Biochemical characterization of exoribonuclease encoded by SARS coronavirus. J Biochem Mol Biol **40:**649–655. http://dx.doi.org/10.5483/BMBRep.2007.40.5.649.
23. **Chen Y, Cai H, Pan J, Xiang N, Tien P, Ahola T, Guo D.** 2009. Functional screen reveals SARS coronavirus nonstructural protein nsp14 as a novel cap N7 methyltransferase. Proc Natl Acad Sci U S A **106:**3484–3489. http://dx.doi.org/10.1073/pnas.0808790106.
24. **Ivanov KA, Hertzig T, Rozanov M, Bayer S, Thiel V, Gorbalenya AE, Ziebuhr J.** 2004. Major genetic marker of nidoviruses encodes a replicative endoribonuclease. Proc Natl Acad Sci U S A **101:**12694–12699. http://dx.doi.org/10.1073/pnas.0403127101.
25. **Decroly E, Imbert I, Coutard B, Bouvet M, Selisko B, Alvarez K, Gorbalenya AE, Snijder EJ, Canard B.** 2008. Coronavirus nonstructural protein 16 is a cap-0 binding enzyme possessing (nucleoside-2′O)-methyltransferase activity. J Virol **82:**8071–8084. http://dx.doi.org/10.1128/JVI.00407-08.
26. **Bouvet M, Debarnot C, Imbert I, Selisko B, Snijder EJ, Canard B, Decroly E.** 2010. In vitro reconstitution of SARS-coronavirus mRNA cap methylation. PLoS Pathog **6:**e1000863. http://dx.doi.org/10.1371/journal.ppat.1000863.
27. **Decroly E, Debarnot C, Ferron F, Bouvet M, Coutard B, Imbert I, Gluais L, Papageorgiou N, Sharff A, Bricogne G, Ortiz-Lombardia M, Lescar J, Canard B.** 2011. Crystal structure and functional analysis of the SARS-coronavirus RNA cap 2′-O-methyltransferase nsp10/nsp16 complex. PLoS Pathog **7:**e1002059. http://dx.doi.org/10.1371/journal.ppat.1002059.
28. **Chen Y, Su C, Ke M, Jin X, Xu L, Zhang Z, Wu A, Sun Y, Yang Z, Tien P, Ahola T, Liang Y, Liu X, Guo D.** 2011. Biochemical and structural insights into the mechanisms of SARS coronavirus RNA ribose 2′-O-methylation by nsp16/nsp10 protein complex. PLoS Pathog **7:**e1002294. http://dx.doi.org/10.1371/journal.ppat.1002294.
29. **Chen Y, Tao J, Sun Y, Wu A, Su C, Gao G, Cai H, Qiu S, Wu Y, Ahola T, Guo D.** 2013. Structure-function analysis of severe acute respiratory syndrome coronavirus RNA cap guanine-N7-methyltransferase. J Virol **87:**6296–6305. http://dx.doi.org/10.1128/JVI.00061-13.
30. **Ke M, Chen Y, Wu A, Sun Y, Su C, Wu H, Jin X, Tao J, Wang Y, Ma X, Pan JA, Guo D.** 2012. Short peptides derived from the interaction domain of SARS coronavirus nonstructural protein nsp10 can suppress the 2′-O-methyltransferase activity of nsp10/nsp16 complex. Virus Res **167:**322–328. http://dx.doi.org/10.1016/j.virusres.2012.05.017.
31. **Jin X, Chen Y, Sun Y, Zeng C, Wang Y, Tao J, Wu A, Yu X, Zhang Z, Tian J, Guo D.** 2013. Characterization of the guanine-N7 methyltransferase activity of coronavirus nsp14 on nucleotide GTP. Virus Res **176:**45–52. http://dx.doi.org/10.1016/j.virusres.2013.05.001.
32. **Pan J, Peng X, Gao Y, Li Z, Lu X, Chen Y, Ishaq M, Liu D, Dediego ML, Enjuanes L, Guo D.** 2008. Genome-wide analysis of protein-protein interactions and involvement of viral proteins in SARS-CoV replication. PLoS One **3:**e3299. http://dx.doi.org/10.1371/journal.pone.0003299.
33. **Roth-Cross JK, Bender SJ, Weiss SR.** 2008. Murine coronavirus mouse hepatitis virus is recognized by MDA5 and induces type I interferon in brain macrophages/microglia. J Virol **82:**9829–9838. http://dx.doi.org/10.1128/JVI.01199-08.
34. **Yang J, Sun Z, Wang Y, Lv J, Qu D, Ye R.** 2011. Partial deletion in the spike endodomain of mouse hepatitis virus decreases the cytopathic effect but maintains foreign protein expression in infected cells. J Virol Methods **172:**46–53. http://dx.doi.org/10.1016/j.jviromet.2010.12.018.
35. **Egloff MP, Ferron F, Campanacci V, Longhi S, Rancurel C, Dutartre H, Snijder EJ, Gorbalenya AE, Cambillau C, Canard B.** 2004. The severe acute respiratory syndrome-coronavirus replicative protein nsp9 is a single-stranded RNA-binding subunit unique in the RNA virus world. Proc Natl Acad Sci U S A **101:**3792–3796. http://dx.doi.org/10.1073/pnas.0307877101.
36. **Thiel V, Ivanov KA, Putics A, Hertzig T, Schelle B, Bayer S, Weissbrich B, Snijder EJ, Rabenau H, Doerr HW, Gorbalenya AE, Ziebuhr J.** 2003. Mechanisms and enzymes involved in SARS coronavirus genome expression. J Gen Virol **84:**2305–2315.
37. **Lugari A, Betzi S, Decroly E, Bonnaud E, Hermant A, Guillemot JC, Debarnot C, Borg JP, Bouvet M, Canard B, Morelli X, Lecine P.** 2010. Molecular mapping of the RNA Cap 2′-O-methyltransferase activation interface between severe acute respiratory syndrome coronavirus nsp10 and nsp16. J Biol Chem **285:**33230–33241. http://dx.doi.org/10.1074/jbc.M110.120014.
38. **Piantavigna S, McCubbin GA, Boehnke S, Graham B, Spiccia L, Martin LL.** 2011. A mechanistic investigation of cell-penetrating Tat peptides with supported lipid membranes. Biochim Biophys Acta **1808:**1811–1817. http://dx.doi.org/10.1016/j.bbamem.2011.03.002.
39. **Battegay M, Cooper S, Althage A, Banziger J, Hengartner H, Zinkernagel RM.** 1991. Quantification of lymphocytic choriomeningitis virus with an immunological focus assay in 24- or 96-well plates. J Virol Methods **33:**191–198. http://dx.doi.org/10.1016/0166-0934(91)90018-U.
40. **van Hemert MJ, van den Worm SH, Knoops K, Mommaas AM, Gorbalenya AE, Snijder EJ.** 2008. SARS-coronavirus replication/transcription complexes are membrane-protected and need a host factor for activity in vitro. PLoS Pathog **4:**e1000054. http://dx.doi.org/10.1371/journal.ppat.1000054.
41. **Gosert R, Kanjanahaluethai A, Egger D, Bienz K, Baker SC.** 2002. RNA replication of mouse hepatitis virus takes place at double-membrane vesicles. J Virol **76:**3697–3708. http://dx.doi.org/10.1128/JVI.76.8.3697-3708.2002.
42. **Snijder EJ, Bredenbeek PJ, Dobbe JC, Thiel V, Ziebuhr J, Poon LL, Guan Y, Rozanov M, Spaan WJ, Gorbalenya AE.** 2003. Unique and conserved features of genome and proteome of SARS-coronavirus, an early split-off from the coronavirus group 2 lineage. J Mol Biol **331:**991–1004. http://dx.doi.org/10.1016/S0022-2836(03)00865-9.
43. **Roth-Cross JK, Martinez-Sobrido L, Scott EP, Garcia-Sastre A, Weiss SR.** 2007. Inhibition of the alpha/beta interferon response by mouse hepatitis virus at multiple levels. J Virol **81:**7189–7199. http://dx.doi.org/10.1128/JVI.00013-07.
44. **Cervantes-Barragan L, Zust R, Weber F, Spiegel M, Lang KS, Akira S, Thiel V, Ludewig B.** 2007. Control of coronavirus infection through plasmacytoid dendritic-cell-derived type I interferon. Blood **109:**1131–1137.
45. **Cervantes-Barragan L, Kalinke U, Zust R, Konig M, Reizis B, Lopez-Macias C, Thiel V, Ludewig B.** 2009. Type I IFN-mediated protection of macrophages and dendritic cells secures control of murine coronavirus infection. J Immunol **182:**1099–1106. http://dx.doi.org/10.4049/jimmunol.182.2.1099.